



UNIVERSITY OF LEEDS

This is a repository copy of *Reconstruction of 3D eolian-dune architecture from 1D core data through adoption of analogue data from outcrop*.

White Rose Research Online URL for this paper:
<http://eprints.whiterose.ac.uk/82576/>

Version: Accepted Version

Article:

Romain, HG and Mountney, NP (2014) Reconstruction of 3D eolian-dune architecture from 1D core data through adoption of analogue data from outcrop. *American Association of Petroleum Geologists (AAPG) Bulletin*, 98 (1). 1 - 22. ISSN 0149-1423

<https://doi.org/10.1306/05201312109>

Reuse

Unless indicated otherwise, fulltext items are protected by copyright with all rights reserved. The copyright exception in section 29 of the Copyright, Designs and Patents Act 1988 allows the making of a single copy solely for the purpose of non-commercial research or private study within the limits of fair dealing. The publisher or other rights-holder may allow further reproduction and re-use of this version - refer to the White Rose Research Online record for this item. Where records identify the publisher as the copyright holder, users can verify any specific terms of use on the publisher's website.

Takedown

If you consider content in White Rose Research Online to be in breach of UK law, please notify us by emailing eprints@whiterose.ac.uk including the URL of the record and the reason for the withdrawal request.



eprints@whiterose.ac.uk
<https://eprints.whiterose.ac.uk/>

1 **Reconstruction of 3D eolian-dune architecture from 1D core data** 2 **through adoption of analogue data from outcrop**

3

4 Hollie Romain¹ & Nigel P. Mountney¹

5 1 – Fluvial & Eolian Research Group, School of Earth and Environment, University of Leeds, Leeds,
6 LS2 9JT, UK

7 **Introduction**

8 Exploration and asset appraisal teams working in hydrocarbon companies typically
9 have access to a varied set of data derived from core and well-log investigations
10 relating to the sedimentology of deposits that make up potential subsurface reservoir
11 intervals. However, at the sub-seismic scale, such datasets are almost exclusively
12 one-dimensional in form, meaning that determination of sedimentary system type
13 and elucidation of the three-dimensional geometry of the various architectural
14 elements present in a reservoir volume, and their reciprocal relationships to one
15 another, are usually highly subjective, resulting in potentially ambiguous
16 interpretations and the postulation of equivocal depositional models (Kocurek 1988;
17 Schenk, 1990; North & Prosser, 1993; North & Boering, 1999). This is especially true
18 for eolian reservoir intervals where the ability to reliably correlate between
19 neighboring wells – even those spaced only a few hundred meters apart, such as
20 deviated sidetracks – is severely hindered by the absence of beds or bounding
21 surfaces that can demonstrably be shown to serve as reliable markers for correlation
22 purposes (Mountney, 2006a). In many cases, the inability to even establish the
23 presence of features regarded to be reliable indicators of paleo-horizontal in

24 preserved eolian reservoir successions is highly problematic (Kocurek, 1988, 1991).
25 This presents difficulties when estimating volumetric sand content and regional
26 porosity-permeability distributions for eolian reservoirs, where the geometries of the
27 various dune, interdune and extradune elements present within the overall three-
28 dimensional rock volume are poorly constrained in the subsurface (e.g. Nagtegaal,
29 1979; Heward, 1991).

30 The aim of this study is to demonstrate how a suite of predictable sedimentological
31 features present in eolian successions can be used to relate detailed sedimentary
32 architectural relationships observable in core and well-log data to the larger-scale
33 sedimentological elements of eolian dune and interdune successions to enable the
34 gross-scale reconstruction of eolian architecture, including estimates of bedform and
35 interdune type, and bedform height, wavelength and spacing. Specific objectives of
36 this study are as follows: (i) to describe the small-scale stratigraphic relationships
37 expected for various different types of eolian bedform morphologies and their
38 resultant preserved deposits arising as a product of eolian bedform migration and
39 accumulation; (ii) to show how the sedimentological attributes of modern eolian
40 systems and ancient outcrop successions can be used to quantify predictable trends
41 in small-scale eolian architecture, and to demonstrate the style of occurrence of
42 these features within larger scale elements (Figure 1); and (iii) to develop and
43 demonstrate a workflow to enable first-order reconstruction of original dune and
44 interdune morphology and preserved three-dimensional architecture from
45 measurements made directly from the limited data provided by one-dimensional
46 cores and well-logs through employment of a series of empirical relationships.

47 Eolian dunes of different morphological type exhibit varying yet predictable
48 configurations of primary depositional facies (principally packages of grainflow, wind-

49 ripple and grainfall strata) and associations of such facies (Hunter, 1977a, b, 1981;
50 Kocurek & Dott, 1981). The distribution of associations of these facies tends to vary
51 predictably over the surface of individual modern eolian bedforms as a function of
52 the various eolian processes that operate on the flank, lee-slope, stoss-slope and
53 brink areas of bedforms (Hunter, 1977a), meaning that primary lithological
54 characteristics such as grain-size distribution, grain packing, and styles of small-
55 scale lamination are also predictable (Livingstone, 1987).

56 In most systems, the mechanics by which eolian bedforms and their constituent
57 stratal packages of associated facies undergo accumulation is dictated by the style
58 by which bedforms undertake migration synchronously with a rise in the
59 accumulation surface (Kocurek, 1988; Kocurek & Havholm, 1993), leading to
60 bedform climbing (Rubin & Hunter, 1982) and the accumulation of sets of cross
61 strata. Although several alternative mechanisms for the accumulation and
62 preservation of sets of eolian strata have been proposed, including the infilling of
63 localized accommodation space (e.g. Langford et al., 2008; Luzón et al., 2012),
64 accumulation around relic eolian topography (Fryberger, 1986), and exceptional
65 bedform preservation following rapid inundation by water or lava flows (e.g. Glennie
66 & Buller, 1983; Mountney et al., 1999; Benan & Kocurek, 2000), the “bedform
67 climbing” mechanism remains a convincing explanation for the origin of the majority
68 of ancient preserved eolian dune successions (Mountney, 2012).

69 Importantly, accumulation of sets of eolian strata via the climbing of bedforms over
70 one another means that typically only the lowermost flanks of migrating bedforms
71 undergo accumulation and preservation into the long-term rock record, whereas the
72 upper parts of bedforms (in most cases the upper 90% or more of a bedform) are
73 truncated by the advance of the following bedform in the train (Rubin & Carter,

74 2006), with the majority of the original dune sediment being reworked (Figure 2).
75 Thus, the proportion and distribution of primary lithofacies preserved in successions
76 in the ancient record does not necessarily reflect the proportion and distribution of
77 primary lithofacies present in modern bedforms. Care must therefore be exercised
78 when using modern bedforms as analogues with which to make predictions about
79 likely facies distributions in reservoir successions. Methods for the accurate
80 prediction and characterization of zones of good reservoir quality in subsurface
81 eolian successions require a clear understanding of the geometry of the various
82 preserved architectural elements and the distribution of packages of facies
83 associated within these elements.

84 Architectural elements (i.e. three-dimensional sediment bodies with specific internal
85 facies characteristics) form the building blocks of eolian reservoir successions and,
86 in most examples, both the elements themselves and the lithofacies of which they
87 are composed internally exhibit a strong preferred directional heterogeneity due to
88 the inherent preferred orientation of layering of laminations and beds of facies, often
89 in a complex nested manner (Weber, 1987; Chandler et al., 1989; Krystinik, 1990).
90 Understanding the detailed arrangement of the style of heterogeneity present in
91 these elements is crucial for reservoir prediction as this exerts a primary control on
92 porosity and permeability structure within eolian reservoirs and therefore dictates
93 production flow rates and patterns within complex eolian reservoir bodies
94 (Nagtegaal, 1979; Heward, 1991; Ellis, 1993; Stanistreet & Stollhofen, 2002; Garden
95 et al., 2005; Bloomfield et al., 2006). In most eolian hydrocarbon plays, it is
96 particularly important to target those intervals within a reservoir that contain a high
97 proportion of grainflow laminae – the deposits of avalanching down dune lee slopes
98 – as these tend to form packages of well-sorted, loosely-packed sandstone with

99 permeabilities that are typically one or more orders of magnitude greater than those
100 in packages of grainfall and wind-ripple strata that dominate in other eolian elements
101 (Chandler et al., 1989; Prosser & Maskall, 1993; Howell & Mountney, 2001).

102 **Background**

103 Since the late 1970s, considerable eolian sedimentological research has focused on
104 large scale stratigraphic relationships and the development of sequence stratigraphic
105 models with which to account for the origin of the eolian record in terms of external
106 controls on sedimentation (e.g. Brookfield, 1977; Kocurek, 1988; Kocurek &
107 Havholm, 1993; Mountney, 2012). As a result of this emphasis, a wide variety of data
108 have been published relating to large-scale stratigraphic architectures preserved in a
109 number of ancient eolian successions (e.g. Glennie & Provan, 1990; Herries, 1993;
110 Mountney & Thompson, 2002; Mountney & Jagger, 2004; Taggart et al., 2010).
111 However, there remain relatively few studies that have investigated the sedimentary
112 style of small-scale dune elements and the arrangement of facies present within
113 preserved eolian sets originating from the migration of different types of eolian
114 bedforms (Ellwood et al., 1975; Hunter, 1977a, b; Kocurek & Dott, 1981; Fryberger &
115 Schenk, 1988). Although some explanation has been offered to account for how
116 such types of small-scale stratification impact on reservoir quality (Lindquist, 1988;
117 Chandler et al., 1989; Prosser & Maskall, 1993; Cox, 1994; Howell & Mountney,
118 2001; Stanistreet & Stollhofen, 2002; Garden et al., 2005; Bloomfield et al., 2006), an
119 effective method to relate deposits seen in one-dimensional core to larger-scale
120 architectural elements has yet to be fully developed.

121 Prediction of facies variability in three dimensions is a key requirement for
122 quantitative reservoir characterization (e.g. Sweet et al., 1996; Fischer et al., 2007)

123 because it enables reliable predictions to be made of the characteristics of a
124 subsurface eolian reservoir bodies such as the extent, type and pattern of
125 distribution of heterogeneities away from the points of data control provided by
126 subsurface wells (Pryor, 1973). For the majority of eolian reservoirs, production
127 behavior and characteristics are primarily influenced and controlled by original
128 sediment fabric (grain size distribution), though secondary alteration of sediment
129 fabric by diagenesis is also important (e.g. Mou & Brenner, 1982). A method to
130 enable the prediction of the spatial occurrence of the original depositional processes
131 that occurred on dunes and in interdunes, and the resultant distribution of lithofacies
132 in preserved eolian architectural elements is therefore essential (Lewis & Couples,
133 1993).

134 Given that most eolian reservoirs are penetrated by a relatively small number of
135 wells and that the typical spacing of these wells is many hundreds of meters to
136 several kilometers, traditional subsurface lithostratigraphic correlation techniques
137 involving the tracing of key stratal surfaces and depositional units are not typically
138 possible. Instead, a commonly adopted method with which to adequately account for
139 facies architecture and with which to predict the scale over which variations in
140 architecture occur is to employ one or more outcrop analogues to provide proxy data
141 (Weber, 1987; Lewis & Rosvoll, 1991, Howell & Mountney, 2001). Such outcrop-
142 analogue studies are important because they provide a method by which regional
143 three-dimensional facies distributions known from outcrop can be used to populate a
144 reservoir volume and thereby inform detailed characterizations and minimize risk.
145 Key to the successful application of this technique is the ability to fit the sedimentary
146 architecture of the chosen outcrop analogue to available core and well-log data from
147 the subsurface reservoir.

148 An inherent problem with reservoir modeling from core and well-log data alone is that
149 such data-types are essentially one-dimensional in form and establishing the most
150 likely three-dimensional sedimentary architecture from such data is typically
151 equivocal (Lindquist, 1988; Luthi & Banavar, 1988; North & Boering, 1999).
152 However, several parameters that effectively define the morphology and geometry of
153 eolian bedforms and their preserved bedsets can be measured directly from
154 subsurface core and these provide a method to directly relate the subsurface
155 architecture present in reservoir successions to outcrop successions for which
156 larger-scale three-dimensional architectural configurations can be determined.

157 Parameters that can be measured directly from core include: (i) preserved set
158 thickness, which for bedsets that originated via bedform climbing is a function of both
159 original bedform wavelength and the angle at which the bedforms climbed over one
160 another as accumulation proceeded (Mountney & Howell, 2000); (ii) the thickness of
161 grainflow units arising from individual sandflow avalanches, which is primarily a
162 function of the length of the lee slope of the original bedform down which
163 avalanching grains of sand cascaded to generate the deposit (Kocurek & Dott, 1981;
164 Howell & Mountney, 2001); (iii) the shape of dune toesets and their style of
165 interaction with deposits of underlying interdune elements, which is an indicator of
166 the style of advance of the original bedform over a neighboring interdune area (e.g.
167 Pulvertaft, 1985; Mountney & Thompson, 2002); (iv) the rate of upward steepening of
168 foresets within a set, which is an indicator of the profile of the lower flanks of the
169 original bedform (Rubin, 1987); (v) the distribution of primary lithofacies (grainflow,
170 wind-ripple and grainfall) within sets, which is a function of processes that operated
171 on the lee slope of the original bedform (Hunter 1977a, b; Kocurek & Dott, 1981);
172 and (vi) the distribution of the occurrence of reactivation surfaces within cosets,

173 which is an indicator of the periodicity with which the original bedforms undertook
174 changes in lee-slope steepness, asymmetry, or migration direction (Rubin, 1987;
175 Fryberger, 1993).

176 Within the remit of this study, detailed examination of the relationships arising
177 between preserved set thicknesses and the thickness of preserved grainflow units
178 has been undertaken. By relating quantitative measurements of these attributes from
179 subsurface core intervals to equivalent sedimentary features observed in exposed
180 outcrop successions, a workflow has been established for the quantification of
181 larger-scale three-dimensional subsurface eolian architecture from limited one-
182 dimensional core data through a suite of empirical relationships. Although the
183 empirical relationships derived from this study serve as useful tools for generalized
184 prediction of sedimentary architecture, application of such relationships should be
185 undertaken with caution: relationships between many measured parameters record
186 significant variability meaning that R^2 values determined for best-fit trend lines are
187 low and not statistically significant in many instances, chiefly as a result of the
188 variability inherent in natural depositional systems such as those studied in this work.

189 Despite these shortcomings, the data show a series of relationships that are
190 nevertheless useful as a basis for a generalized technique to reconstruct the three-
191 dimensional architecture from primary depositional facies in eolian successions.
192 Specifically, the empirical relationships presented herein are useful for the
193 determination of trends between features observable in core and several aspects of
194 wider three-dimensional sedimentary architecture that cannot be determined by
195 direct observation from subsurface datasets. Thus, such trends are useful for making
196 first-order predictions of the likely internal three-dimensional sedimentary
197 architectures of subsurface reservoir successions and can be used to assist in the

198 construction of reservoir models for the prediction of porosity-permeability
199 distributions and likely flow properties.

200 For example, in successions interpreted to have arisen in response to the migration
201 and aggradation of large linear dune bedforms, a vertical stacking of thick packages
202 of relatively low-angle-inclined, wind-ripple-dominated packages of strata is common,
203 with only the uppermost parts of sets having foresets that steepen upward
204 sufficiently to preserve grainflow strata (Krystinik, 1990). Determining the proportions
205 of wind-ripple and grainflow strata and the distribution of their occurrence within
206 preserved sets is key to understanding the three-dimensional configuration of
207 packages of facies, and this is most readily achieved through comparison to
208 analogous outcrop examples.

209 **Data and Methods**

210 To establish a suite of empirical relationships between eolian sedimentary
211 parameters that can be measured directly from both one-dimensional core and from
212 the larger-scale eolian architectural elements observable from outcrop successions,
213 data have been collected from the Permian Cedar Mesa Sandstone and Jurassic
214 Navajo Sandstone, two eolian successions that are well exposed in the South East
215 Utah area, U.S.A. Four localities were studied in the so-called erg center region of
216 the Permian Cedar Mesa Sandstone succession (Mountney, 2006b) in the White
217 Canyon and Hite areas and an additional three localities were studied in the so-
218 called erg margin region at Squaw Butte, Salt Creek Butte and Mosquito Butte
219 (Figure 3a). Four localities were also studied in the Jurassic Navajo Sandstone in the
220 area around the town of Moab, Utah (Figure 3b), which represents an erg center
221 setting within the paleo-erg system (Blakey & Ranney, 2008).

222 Primary measurements of eolian bedset architectures were made at each study
223 locality to determine three-dimensional relationships present in the successions of
224 eolian dune sets. Aspects of eolian architecture measured included: (i) maximum
225 preserved set thicknesses for 42 individual trough cross-bedded sets exposed in
226 orientations both parallel and perpendicular to eolian transport direction (itself
227 determined through analysis of dip-azimuth data relating to grainflow deposits
228 representative of accumulation on the slipface of the original bedforms) – care was
229 taken to account for set-thickness variations arising from the curved nature of trough
230 cross-bedded sets; (ii) geometries of packages of grainflow strata representative of
231 individual lee-slope sand avalanches, including thickness (932 readings in total),
232 width (30 readings in total) and length (517 readings in total); (iii) measurements of
233 bedform wavelength (42 readings in total) determined in directions parallel to eolian
234 paleo-transport mostly by the measurement of the spacing between the points at
235 which successive interdune migration surfaces climb off basal supersurfaces that are
236 themselves inferred to represent paleohorizontal surfaces (see Mounney & Howell,
237 2000 and Mounney, 2006b for details of the methodology); (iv) measurements of
238 angles of set climb (42 readings in total), determined trigonometrically in directions
239 parallel to eolian paleo-transport (again determined through analysis of dip-azimuth
240 data relating to grainflow deposits representative of accumulation on the slipface of
241 the original bedforms) by evaluating the rate of rise of interdune migration surfaces
242 relative to underlying supersurfaces (see Mounney, 2006b for methodology); (v)
243 measurements of the rate of upward steepening of eolian dune toset deposits with
244 increasing height above the base of sets (36 readings in total).

245 **Results**

246 Grainflow Geometry

247 The mean lengths and widths of single units of grainflow strata in the Navajo
248 Sandstone are 4.22 m (standard deviation = 2.43; n = 517) (Figure 4a), and 4.63 m
249 (standard deviation = 1.58; n = 30) (Figure 4b), respectively. Grainflow width data
250 were not measured from the Cedar Mesa Sandstone. The mean thicknesses of
251 single units of grainflow strata (i.e. deposits representative of a single sandflow
252 avalanche event) in the Navajo Sandstone and Cedar Mesa Sandstone are 23.77
253 mm (standard deviation = 7.32; n = 517), and 54.68 mm (standard deviation = 23.11;
254 n = 415), respectively (Figure 4c). Individual grainflow units have been identified by
255 their subtle inverse grading, which gives rise to a sharp grain-size contrast across
256 unit boundaries that typically takes the form of a change from lower to upper fine-
257 grained sand. Additionally, these units are in many instances identified by their style
258 of interfingering and intercalation with thin accumulations of wind-ripple strata,
259 especially in the lower parts of preserved sets, and with thin accumulations of
260 grainfall strata, most notably in the upper parts of preserved sets.

261 Preserved Set Thickness

262 Preserved set thicknesses have been measured from the central axes of troughs
263 (i.e. at the location of the thickest development of the set). The mean thicknesses of
264 simple preserved sets (*sensu* McKee, 1979) of strata bounded by interdune
265 migration bounding surfaces in the Navajo Sandstone and Cedar Mesa Sandstone
266 are 3.10 m (standard deviation = 1.60; n = 25), and 4.71 m (standard deviation =
267 2.72; n = 17), respectively (Figure 4d). For the Cedar Mesa Sandstone, measured
268 set thicknesses are representative of the succession overall, though considerable
269 variability exists in some locations. For the Navajo Formation, which is exposed over

270 large areas of Utah, Arizona and Colorado, preserved set thicknesses vary
271 considerably and the sets measured as part of this study from parts of the
272 succession exposed around the town of Moab, Utah, are not necessarily
273 representative of the formation overall. Indeed, significantly thicker compound sets
274 are known from other parts of this formation (see, for example, Herries, 1993 and
275 Rubin, 1987), though these have not been examined for this study.

276 Bedform Wavelength Reconstruction

277 Original dune wavelengths were mostly determined via direct measurement. In
278 directions parallel to eolian paleo-transport, the spacing between the points at which
279 successive interdune migration surfaces climb off basal supersurfaces that are
280 themselves inferred to represent paleohorizontal surfaces is a measure of bedform
281 spacing, where bedform spacing is defined as the bedform wavelength plus the
282 additional component of width of any adjoining interdune flat. Additional calculations
283 of original dune wavelengths were derived trigonometrically from estimates of set
284 thicknesses and angles of climb: see Mountney & Howell (2000) for details of the
285 method. The mean reconstructed dune bedform wavelengths in directions parallel to
286 inferred eolian bedform migration direction for studied parts of the Navajo Sandstone
287 and Cedar Mesa Sandstone are 138.26 m (standard deviation = 70.75; n = 25), and
288 202.42 m (standard deviation = 159.19; n = 15), respectively (Figure 4e).

289 Based on relationships observed from Navajo Sandstone, where sets are seen to
290 rise (climb) off supersurfaces, reconstructed dune bedforms are estimated to have
291 had original wavelengths ranging from 80 to 340 m. The erg center region of the
292 Cedar Mesa Sandstone exhibits a wider range of reconstructed dune wavelength
293 values (65 m to 668 m). Overall, these data fall within the ranges determined

294 previously for eolian dunes of the Cedar Mesa Sandstone in the White Canyon
295 region of SE Utah (Mountney, 2006b). However, one exception is Set 1 from Mile
296 101 of Highway 95 (a 12.8 m-thick set climbing at an angle of 1.1°), which is
297 estimated to represent the preserved deposit of a bedform that had an anomalously
298 large wavelength of 668 m, considerably greater than values determined for other
299 bedforms in the succession.

300 Angle of Climb

301 The Navajo Sandstone exhibits a narrow range of observed angles of climb, with the
302 majority of sets climbing up through the stratigraphy in a downwind direction at
303 angles between 1 to 1.5°. The mean angle of climb of studied sets in the Navajo
304 Sandstone is 1.29° (standard deviation = 0.30; n = 25). Sets in the erg center region
305 of the Cedar Mesa Sandstone reveal a wider range of climb angles, which were
306 derived by Mountney (2006b, his Figure 12) trigonometrically from measurements of
307 preserved set thicknesses and reconstructed original dune bedform wavelengths
308 (the latter determined from the spacing between points where sets rise off
309 supersurfaces which themselves define a paleohorizontal surface). The mean angle
310 of climb of studied sets in the Cedar Mesa Sandstone is 1.54° (standard deviation =
311 0.75; n = 17 (Figure 4f).

312 **Discussion**

313 Several important empirical relationships describing relationships between the
314 spatial arrangement of observed lithofacies and the geometry and style of
315 distribution of larger-scale eolian architectural elements are identified from analysis
316 of the field-derived data.

317 Relationship between preserved grainflow thickness, length and width

318 Where the pattern of outcrop has allowed, for every grainflow unit measured in the
319 Navajo Sandstone ($n = 517$), the preserved thickness has been related to a
320 corresponding grainflow length and width (Figures 5 & 6). In the Navajo Sandstone,
321 measured grainflow widths exhibit a strong positive correlation with corresponding
322 grainflow thickness (Figure 5; $y = 0.0041x + 0.0035$; $R^2 = 0.86$). The overall
323 relationship between measured grainflow length and preserved grainflow thickness
324 for sets in the Navajo Sandstone shows a positive correlation but with substantial
325 scatter (Figure 6; $y = 0.0019x + 0.0156$; $R^2 = 0.41$). However, preserved grainflow
326 thickness and length relationships from 25 *individual* sets are also depicted in Figure
327 6 and strong positive correlations between preserved thickness and length exist in
328 almost every case. Significantly, however, data from different sets plot in distinct
329 and, in many cases, non-overlapping fields on the graph. Together, these
330 observations suggest that, although a simple overall general relationship between
331 grainflow thickness and grainflow length exists, data from individual sets each
332 preserve grainflows with their own geometry and this likely reflects the shape of the
333 slipface that developed on the lee of the dune at the time of sedimentation.

334 Empirical relationships identified from outcrop data between grainflow thickness,
335 length and width are important because they potentially allow the three-dimensional
336 reconstruction of the expected geometry of grainflow sediment packages solely from
337 a measurement of their thicknesses preserved in core. This is important for modeling
338 lamina- and bed-scale heterogeneity and directional permeability in eolian reservoirs
339 (Weber, 1982, 1987; Chandler et al., 1989; Krystinik, 1990).

340 Relationship between preserved set thickness, dune wavelength and angle-
341 of-climb

342 In both the Cedar Mesa Sandstone and the Navajo Sandstone, dune-sets generated
343 by the migration and climb of larger bedforms (as determined by reconstructed
344 estimates of longer wavelengths) preserve thicker grainflow units, though
345 considerable spread exists between the data (Figure 7a; Cedar Mesa Sandstone; $y =$
346 $1E-05x + 0.0532$; $R^2 = 0.02$; Navajo Sandstone; $y = 6E-05x + 0.0148$; $R^2 = 0.38$).
347 Although the studied dune-sets from the Navajo Sandstone are indicative of original
348 bedforms characterized by generally smaller wavelengths than those of the Cedar
349 Mesa Sandstone, considerable overlap in original bedform wavelength exists. Of the
350 preserved dune-sets for which estimates of reconstructed original bedform
351 wavelengths are similar, examples from the Navajo Sandstone are characterized by
352 distinctly thinner grainflow units than those from the Cedar Mesa Sandstone (Figure
353 7a). This could have arisen due to a number of reasons: different dune types,
354 different slipface configurations, variations in dune-plinth shape, variations in dune
355 height (a likely influence on slipface length) despite bedforms having similar
356 wavelengths, and different grain-size distributions or grain-shape properties giving
357 rise to different types of avalanches down the dune lee slopes. The overall
358 correlation between preserved grainflow thickness and original bedform wavelength
359 represents a possible method for making a first-order estimate of original bedform
360 size from subsurface data since the former can be measured directly from core.

361 However, the spread of the data and the different trends in the data for the Navajo
362 and Cedar Mesa sandstones demonstrate that it is essential to pick an appropriate

363 analogue when making extrapolations regarding larger-scale architecture from core
364 data.

365 For climbing eolian systems that accumulate a succession through progressive climb
366 of bedforms over one another, preserved set thickness is a function of both bedform
367 size (wavelength) and angle-of-climb (Figure 8; Rubin, 1987; Rubin & Carter, 2006).
368 Despite preserved set thickness being only partly dependent on original dune
369 wavelength, for the studied successions there exists a clear positive relationship
370 between preserved set thickness and dune wavelength (Figure 7b – Cedar Mesa
371 Sandstone - $R^2 = 0.61$; Navajo Sandstone - $R^2 = 0.78$). Note, however, that ignoring
372 the outlier that represents the anomalously large bedform studied in the Cedar Mesa
373 Sandstone reduces the R^2 value for the best-fit line for these data from 0.61 to 0.20.

374 The nature of the relationship between preserved set thickness and dune
375 wavelength is similar for both the Cedar Mesa and Navajo sandstones, principally
376 because sets from both systems in the areas studied are climbing at similar angles
377 (the majority in the range 1 to 1.5°), which means that the effects of angle-of-climb
378 are largely normalized. However, although sets in some other systems are known to
379 climb at similar angles (e.g. Triassic Helsby Sandstone – 1 to 1.5°, Mounthey &
380 Thompson, 2002), others successions climb at lower angles (e.g. the transition zone
381 between the Undifferentiated Cutler Group and the Cedar Mesa Sandstone at Indian
382 Creek, SE Utah – 0.35°, Mounthey & Jagger, 2004) or steeper angles (e.g. parts of
383 the Etjo Sandstone, Namibia – up to 4°, Mounthey & Howell, 2000, as well as
384 examples from some very dry dune systems characterized by small dunes, which
385 have not been addressed in this study). Thus, it is important to consider angle-of-
386 climb when using preserved set thickness to reconstruct likely original bedform size.

387 Although a positive relationship has long been recognized whereby increased climb
388 angles tend to preserve thicker sets (e.g. Mountney & Howell, 2000), such increased
389 angles of climb do not necessarily arise from the accumulation of larger bedforms
390 with longer wavelengths. Indeed, larger bedforms with longer wavelengths tend to
391 undertake accumulation through climb at shallower angles, primarily because larger
392 bedforms are likely to respond only slowly to changes in sand availability and will
393 therefore tend to climb at only shallow angles, though they can preserve relatively
394 thick sets by virtue of their long wavelength. Thus, preserved set thickness alone is
395 not necessarily a reliable indicator of original bedform size.

396 Relationship between preserved set thickness and grainflow thickness

397 For each set for which a thickness has been measured, 15 to 25 grainflow
398 thicknesses have also been measured; the relationship between preserved set
399 thickness and grainflow thickness shows significant scatter (Figure 9; Cedar Mesa
400 Sandstone, $y = 102.09x - 0.9557$, $R^2 = 0.2137$; Navajo Sandstone, $y = 182.79x -$
401 1.2566 , $R^2 = 0.5797$). However, overall results demonstrate a weak positive
402 correlation for data from both studied outcrop successions. Comparable ranges of
403 preserved grainflow thicknesses measured from sets of known thickness were also
404 demonstrated by Howell & Mountney (2001), whose results concluded that there was
405 no apparent significant relationship between preserved set thickness and grainflow
406 thickness for the Cretaceous Etjo Formation of Namibia. Plotting preserved set
407 thicknesses against grainflow thicknesses does not necessarily reveal an obvious
408 correlation for several reasons (Figure 10): (i) set thickness is a function of not only
409 bedform size (wavelength), but also angle-of-climb and set-thickness data collected
410 from multiple eolian successions or from different geographic locations or

411 stratigraphic levels within the same succession will be partly dictated by bedforms
412 that locally climbed at different angles (Figure 10a); (ii) values of set thicknesses
413 determined from two-dimensional outcrops or from one-dimensional core do not
414 necessarily represent the maximum thickness of a set since they might be clipping
415 the edges of troughs that are significantly thicker in their central parts (Figure 10b);
416 (iii) because preserved grainflow units thin and pinch-out laterally, two-dimensional
417 outcrops and one-dimensional core might be clipping the 'thin' edges of grainflow
418 units, thereby not recording their true maximum thickness (Figure 10c); (iv) sets
419 might only preserve the basal-most toes of grainflow units, which typically thin and
420 pinch-out in the lower parts of dune lee slopes as the angle of inclination of the slope
421 decreases (Figure 10d) where packages of wind-ripple strata become dominant.
422 Such situations most commonly arise when seasonally-reversing wind regimes
423 encourage the development of a gently inclined dune plinth at the base of the lee
424 slope (e.g. Rubin, 1987). For these reasons, when analyzing grainflow units in core
425 data for the purpose of reconstructing likely bedform architecture, it is preferable to
426 record data from the thickest sets that are likely most representative of a penetration
427 through the centers of troughs. Within these, the thickest-preserved grainflow units
428 will most closely reflect the maximum developed grainflow thickness, which might
429 provide an indicator of lee slope length and therefore bedform height and overall
430 size; thinner grainflow units will likely record examples where the well bore has
431 intersected grainflows at points close to either their lateral or downslope margins.

432 The Cedar Mesa Sandstone offers the opportunity to examine this problem in more
433 detail because the overall succession in both the erg center setting (e.g. Mile 75 of
434 White Canyon) and in the erg margin setting (e.g. Squaw Butte) is divided into a
435 number of separate eolian erg sequences each bounded both above and below by

436 regionally extensive deflationary supersurfaces (Loope, 1985; Mountney & Jagger,
437 2004; Mountney 2006b). This partitioning into a series of stacked supersurface-
438 bounded eolian sequences means that reliable estimates can be made of both the
439 angle of climb of sets and of original dune wavelength. This provides the basis for a
440 method with which to demonstrate how preserved set thickness is related to
441 grainflow thickness.

442 Preserved set thicknesses plotted against grainflow thicknesses for a number of
443 dune sequences in the erg center and lateral erg margin areas of the Cedar Mesa
444 Sandstone are shown in Figure 11 ($y = 0.2614e^{99.347x}$, $R^2 = 0.6238$). The scatter in
445 the data is less than that shown for the plot in Figure 9 for several reasons: (i) set
446 thicknesses were determined from the centers of troughs (i.e. at their point of
447 maximum thickness), which could be reliably and consistently picked because of the
448 exceptionally high-quality nature of the outcrop; (ii) for each set examined, 10
449 grainflows units were measured at their point of *maximum* thickness and the mean of
450 these 10 values was recorded so as to negate the effects of thinning and pinching of
451 grainflow units at their lateral and downslope margins.

452 Results from the eight individual eolian sequences examined and plotted on Figure
453 11 demonstrate that each exhibits a strong positive correlation between preserved
454 set thickness and grainflow thickness *but* considerable scatter exists *between* each
455 separate eolian sequence if the dataset is considered in its entirety. The origin of the
456 scatter in these data arises partly because preserved set thickness is a function of
457 both angle-of-climb and original bedform wavelength, which varied between each
458 studied eolian sequence. Additionally, grainflow thickness is also known to vary as a
459 function of slipface length, with thicker grainflows developing on longer slipfaces
460 associated with larger bedforms (Kocurek & Dott, 1981). Thus, the strong positive

461 correlation between preserved set thickness and grainflow thickness *within* each
462 sequence indicates a direct relationship between grainflow thickness and bedform
463 size (height), a relationship that is discussed in more detail in the next section.

464 Little overlap exists between the population of data describing reconstructed dune
465 wavelength versus grainflow thickness from the Cedar Mesa and Navajo sandstones
466 (Figure 7a). This demonstrates the importance of identifying and applying the most
467 appropriate outcrop analogue when applying these types of data as a predictive tool
468 with which to reconstruct likely bedform size from subsurface grainflow and set-
469 thickness data recorded in core. Selection of an appropriate analogue should be
470 based on the following: comparable preserved set thicknesses, comparable
471 grainflow thickness distribution, proportion of facies which are comparable (grainflow,
472 wind-ripple and grainfall), the arrangement of such facies, and the variability of
473 foreset azimuth data. Overall, for sets thought to have been generated by dunes with
474 similar wavelengths, the Navajo system has preserved significantly thinner
475 grainflows than the Cedar Mesa system (Figure 7a), probably because the dunes of
476 the two systems had markedly different morphologies with different slipface
477 configurations.

478 Relationship between preserved grainflow thickness and original bedform
479 size (dune height and wavelength)

480 A positive correlation has been demonstrated previously between dune slipface
481 height and the thickness of grainflow units that are generated as a consequence of
482 lee-slope avalanching down such slipfaces in modern, small-to-medium-sized dunes
483 (Kocurek & Dott, 1981) and a similar relationship is noted for data collected as part
484 of this study (Figure 12; Navajo Sandstone, $y = 1532.7x^{1.6006}$, $R^2 = 0.5965$; Kocurek

485 & Dott (1981) dataset, $y = 988.78x^{1.4796}$, $R^2 = 0.5555$). In their initial stages of
486 development, sandflow avalanches thicken as an increasing volume of sand
487 becomes entrained in the flow. For small and medium-sized dunes, grainflow
488 deposits therefore become thicker with increasing slope length and, by implication,
489 bedform height (Kocurek & Dott, 1981). Once fully developed, sandflow avalanches
490 tend to attain an equilibrium thickness and individual preserved grainflow deposits
491 rarely exceed 60 to 80 mm in thickness. Departures from the trend can arise for a
492 number of reasons: (i) successive avalanches may be erosional at their base, such
493 that previously emplaced avalanche deposits are partly reworked by later deposits,
494 thereby reducing preserved grainflow thickness; (ii) deposits of individual grainflows
495 tend to thin to a point of pinch-out at their downslope limit where they interfinger with
496 packages of wind-ripple strata (e.g. Figure 1b), and it is these thinner grainflow
497 deposits that have greater preservation potential in cases where bedform climbing at
498 low angles allows for preservation of only the basal most parts of the original dune
499 lee slope, or where grainflows do not extend to the base of the set (Figure 2b); (iii)
500 the generally well sorted texture of eolian lee-slope deposits means that separate
501 grainflow units might appear as a single apparently homogenous package of sand
502 lacking any internal stratification and such deposits could be misinterpreted as a
503 single anomalously thick avalanche deposit (e.g. "outliers" in Figure 7a and 9).
504 Additionally, the effects of sediment compaction will influence comparisons between
505 modern grainflow deposits and ancient preserved grainflow strata.

506 For many modern bedform types, dune height exhibits a positive correlation with
507 bedform wavelength and spacing (e.g. Wilson, 1973; Lancaster, 1988; Figure 13;
508 simple dunes, $y = 18.944x + 333.56$, $R^2 = 0.0885$; compound dunes, $y = 14.959x +$
509 538.74 , $R^2 = 0.2854$; complex dunes, $y = 8.8474x + 268.74$, $R^2 = 0.3502$). It is

510 therefore possible to demonstrate an indirect relationship between grainflow
511 thicknesses preserved in ancient successions and original bedform height via this
512 relationship between bedform wavelength and height (Figures 7a and 12).
513 Importantly, this means that if grainflow thickness is known solely from subsurface
514 core data, then a first-order estimate of both original bedform height and wavelength
515 can tentatively be suggested. Furthermore, if both bedform wavelength and
516 preserved set thickness are known, then a generalized estimate of the angle of climb
517 of the succession can be made through a simple trigonometric relationship based on
518 the approach outlined by Mountney & Thompson (2002). For this approach to be
519 applied reasonably, care must be taken to determine which type of eolian bedform
520 has been encountered in core, since mis-interpretation can result in errors of up to
521 two orders of magnitude in reconstructed estimates of likely bedform spacing (Figure
522 13). Bedform type (simple, compound or complex) can potentially be deduced from a
523 thick succession of core by ascribing different genetic significance to bounding
524 surfaces of various types (e.g. interdune migration surfaces, superimposition
525 surfaces, reactivation surfaces; see Brookfield, 1977, Rubin, 1987, and Rubin &
526 Carter, 2006, for a summary of the technique).

527 The likely presence of an anomalously large bedform in the Cedar Mesa Sandstone
528 at Mile 101 on Highway 95 (White Canyon) is supported by the relationships of
529 Kocurek & Dott (1981), who suggest that original bedform size can be estimated
530 based on proportions of grainfall strata to grainflow strata in preserved dune sets.
531 Dune sets at Mile 101 preserve no grainfall strata and are composed almost entirely
532 of grainflow strata (95%), with only minor intercalations of wind ripple strata (5%).
533 The average grainflow thickness for this set at Mile 101 is 73 mm, 9mm greater than

534 the average for other sets at this locality, again supporting the interpretation of a
535 large bedform with an unusually high and long slipface.

536 Applied workflow for reconstruction of eolian architecture from core data

537 The series of empirical relationships identified as part of this study enable aspects of
538 small-scale eolian stratigraphy observable in core to be related to larger-scale
539 architectural elements; this potentially allows for the first-order reconstruction of the
540 probable geometry and scale of aeolian bedforms responsible for giving rise
541 preserved eolian accumulations directly from core data. Sedimentological attributes
542 that can be measured directly from core (and in some cases wireline log) data
543 include preserved set thickness, grainflow thickness, shape of dune toesets, rate of
544 upward steepening of foresets within a set, and the distribution of primary lithofacies
545 (grainflow, wind-ripple, and grainfall) within sets. Of these, this study has focused on
546 the establishment of a series of empirical relationships based on measurements of
547 preserved set thickness and grainflow thicknesses within the core sections.

548 For climbing eolian systems that have accumulated and preserved a succession
549 through progressive climb of bedforms over one another, preserved set thickness is
550 a function of both bedform size (wavelength) and the angle of system climb.
551 Although preserved set thickness is only partly dependent on original bedform
552 wavelength, there exists a positive linear relationship between preserved set
553 thickness and reconstructed original bedform wavelength. Fundamental relationships
554 exist between slipface height and thickness of grainflow packages preserved for
555 small to medium dunes and these relationships established from this study of two
556 ancient eolian successions compare closely to a similar relationship established
557 previously for modern dunes (Kocurek & Dott, 1981). Preserved grainflow

558 thicknesses observed in core can be used as a proxy (albeit with some reservations)
559 to predict original bedform height, and therefore size (Figure 12), given that bedform
560 height can be related to bedform wavelength for various types of dunes (Figure 13).
561 If grainflow thickness is known, then an estimate of bedform wavelength can be
562 made. If both original bedform wavelength and preserved set thickness are known,
563 then the angle-of-climb of the succession can be determined using a simple
564 trigonometric method in the absence of high-resolution seismic data. Although
565 steeper angles of system climb preserve thicker sets for the accumulation of
566 bedforms of a given wavelength, steeper angles of climb do not necessarily result
567 from the migration and accumulation of larger dunes with longer wavelengths.

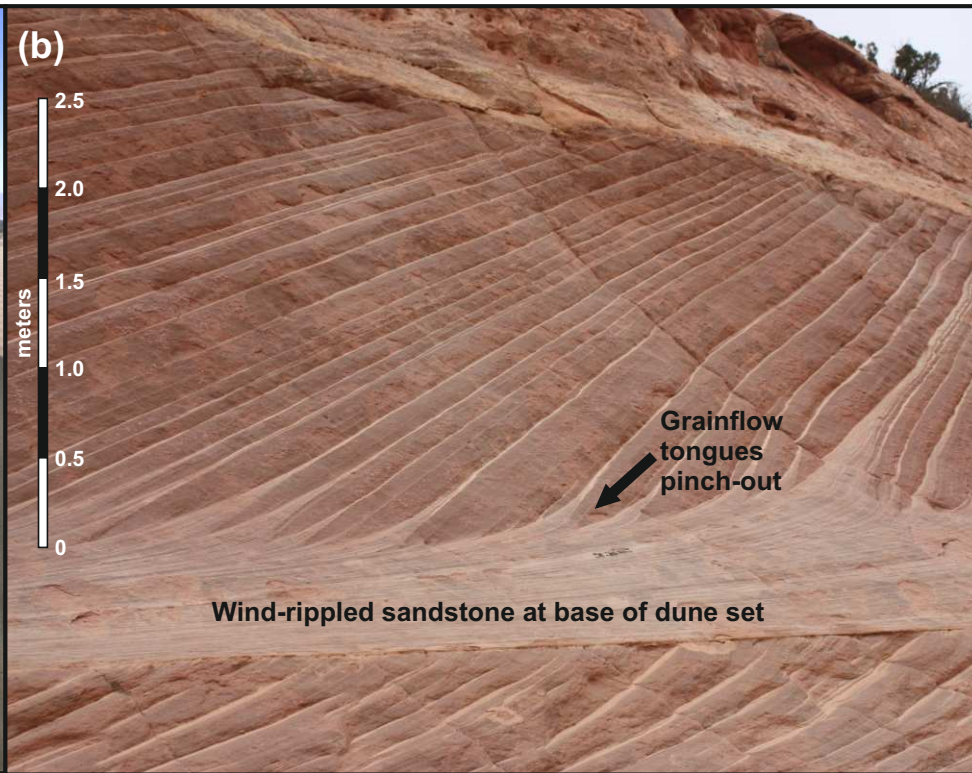
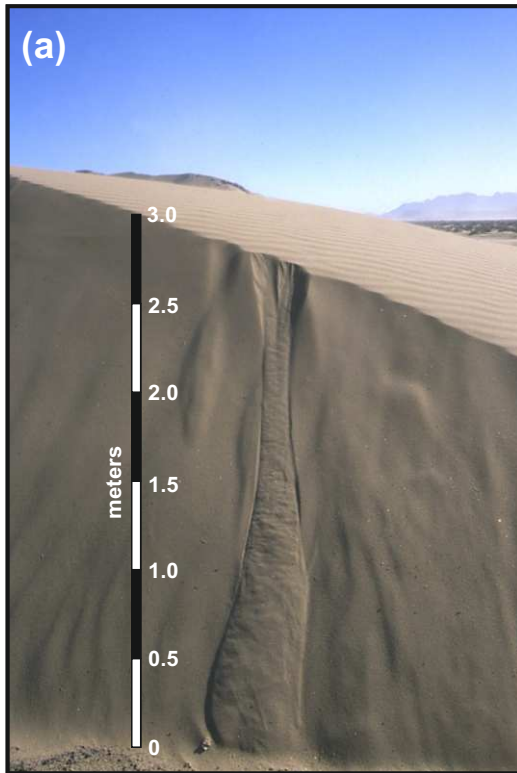
568 **Conclusions**

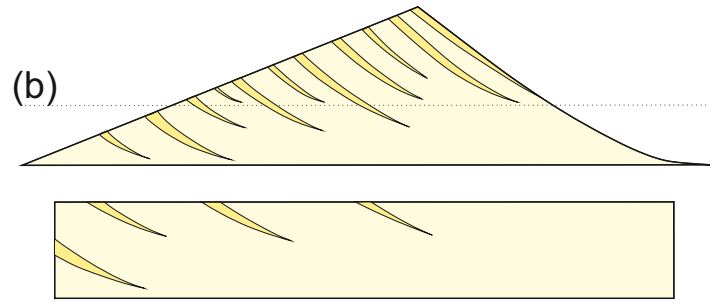
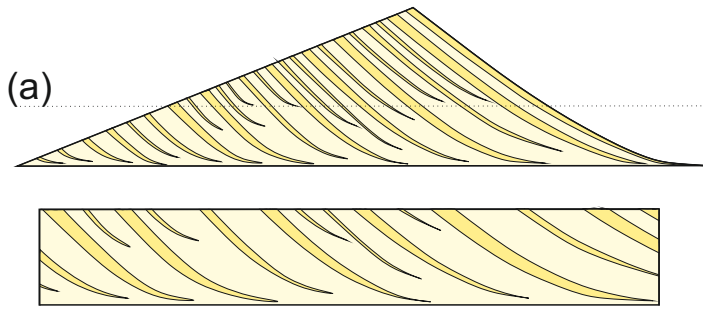
569 A suite of empirical relationships have been developed based on analysis of eolian
570 outcrop data from parts of the Permian Cedar Mesa Sandstone and the Jurassic
571 Navajo Sandstone in SE Utah. These relationships enable parameters measured
572 directly from one-dimensional core to be related to larger scale eolian architectural
573 elements observable in outcrop successions and underpin a simple method for
574 reconstructing eolian geometry from one-dimensional subsurface datasets alone.
575 However, care must be exercised in the application of this technique: as with most
576 statistical data derived from natural datasets, the spread of the data is, in many
577 cases, considerable and significant; resulting in data distributions that yield best-fit
578 trends with low R^2 values that are statistically weak. However, despite these
579 shortcomings, relationships between measurements small- and larger-scale aspects
580 of sedimentary architecture form the basis for the development of a predictive tool
581 that can potentially be applied with care to subsurface datasets for elucidation of

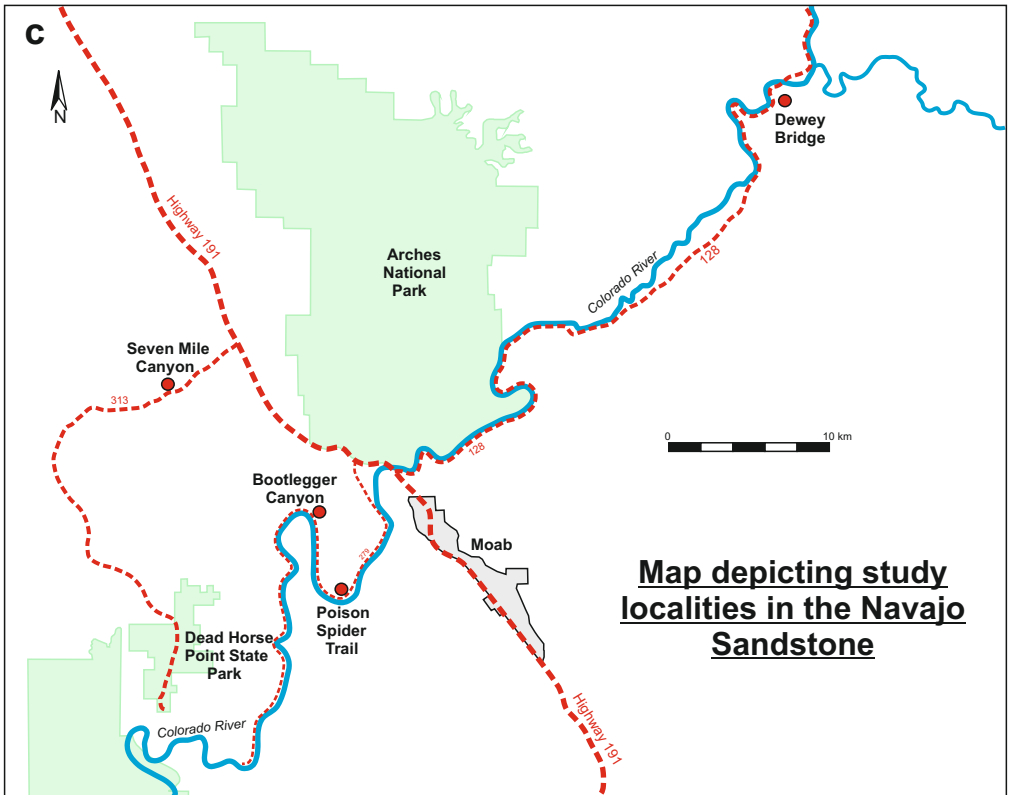
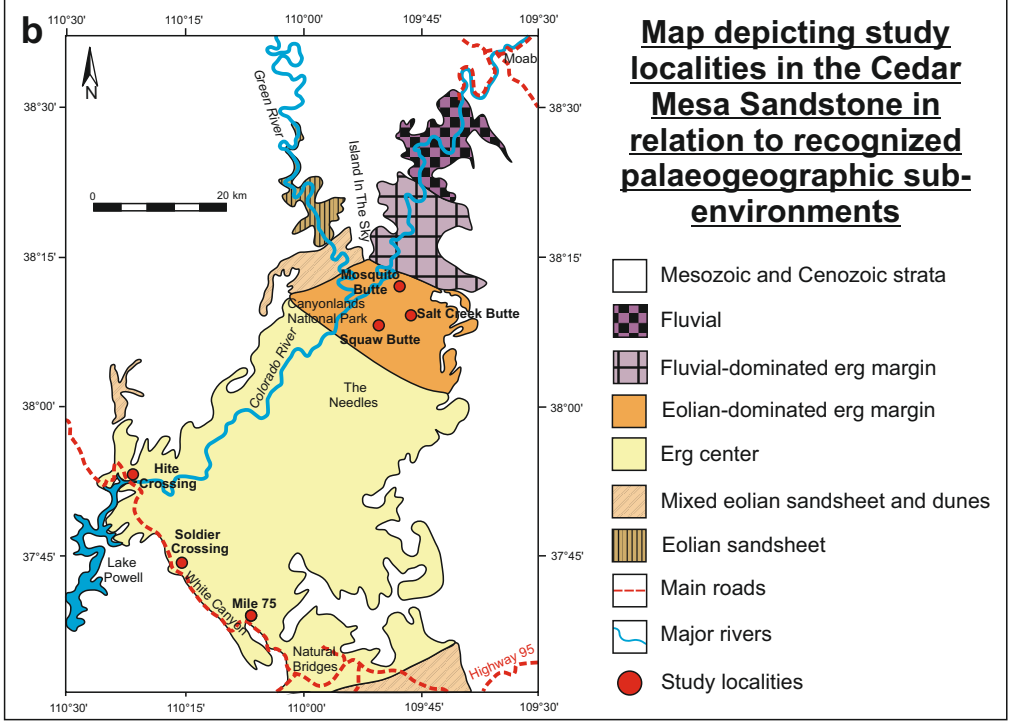
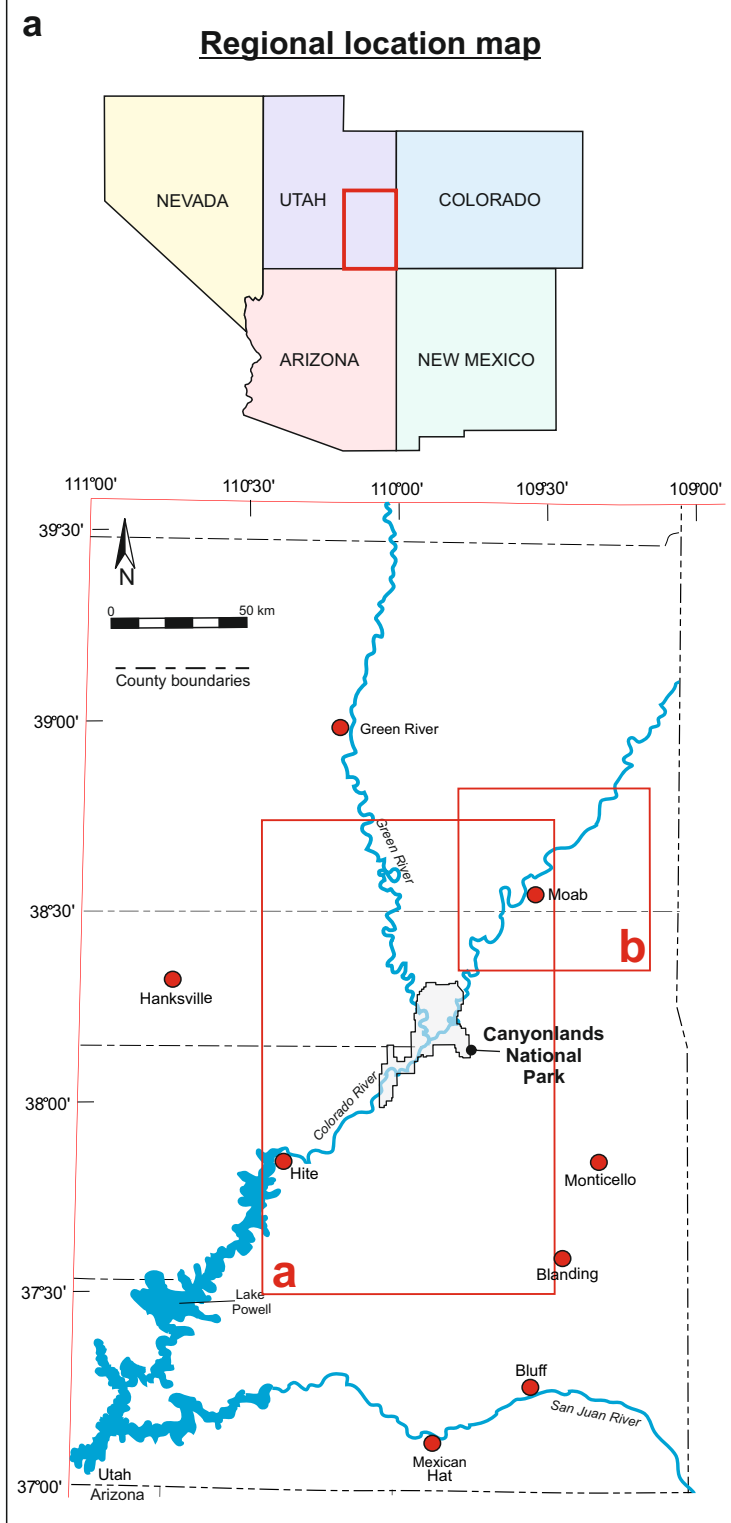
582 larger-scale sedimentary architecture and therefore for prediction of regional
583 reservoir stratigraphic heterogeneity.

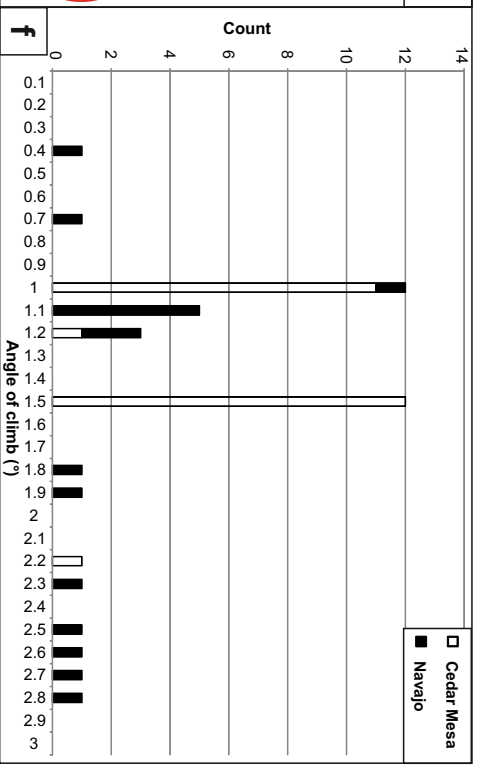
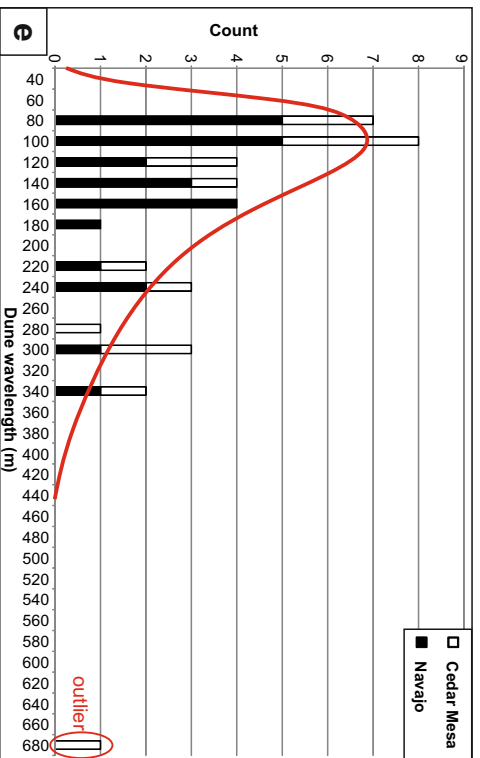
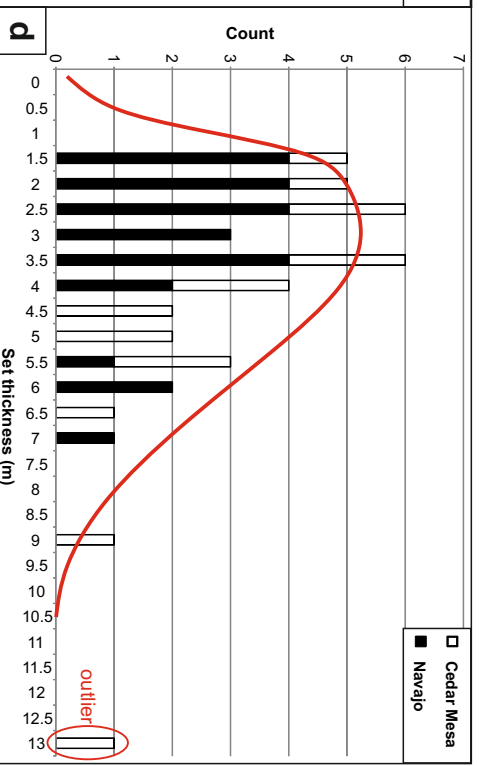
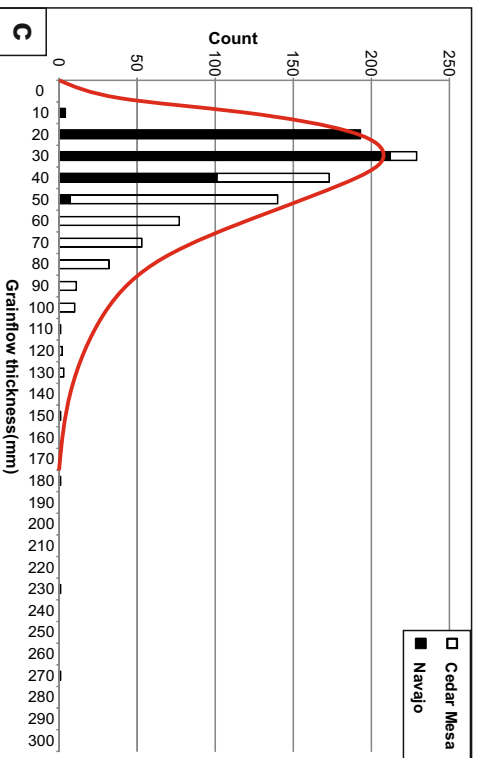
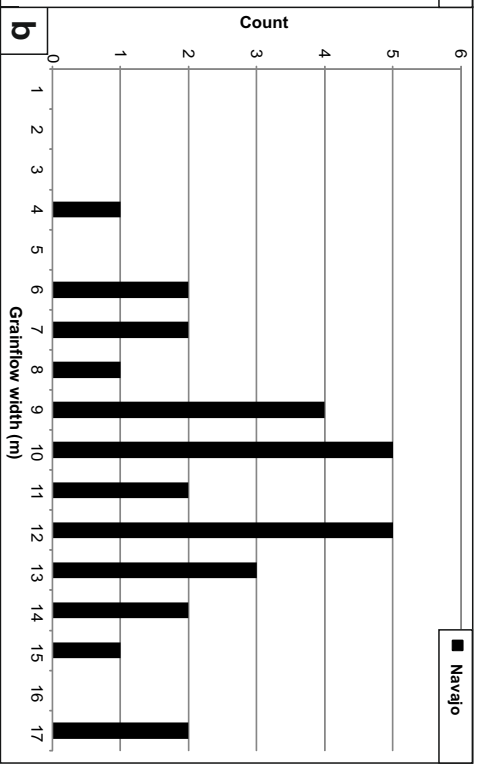
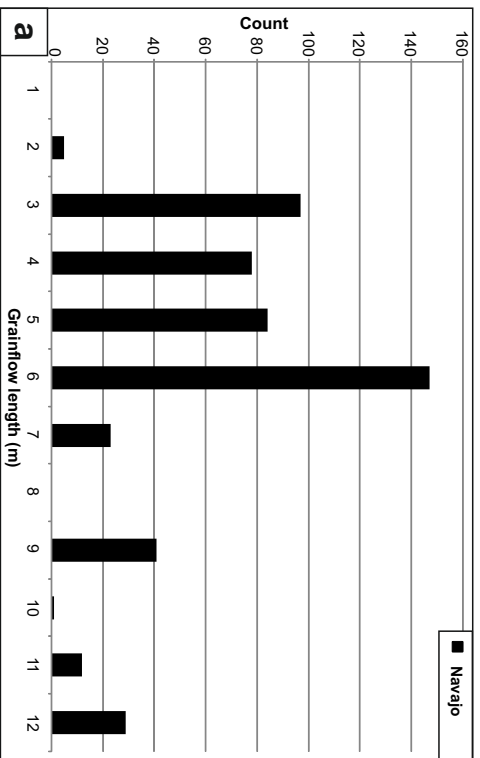
584 **Acknowledgments**

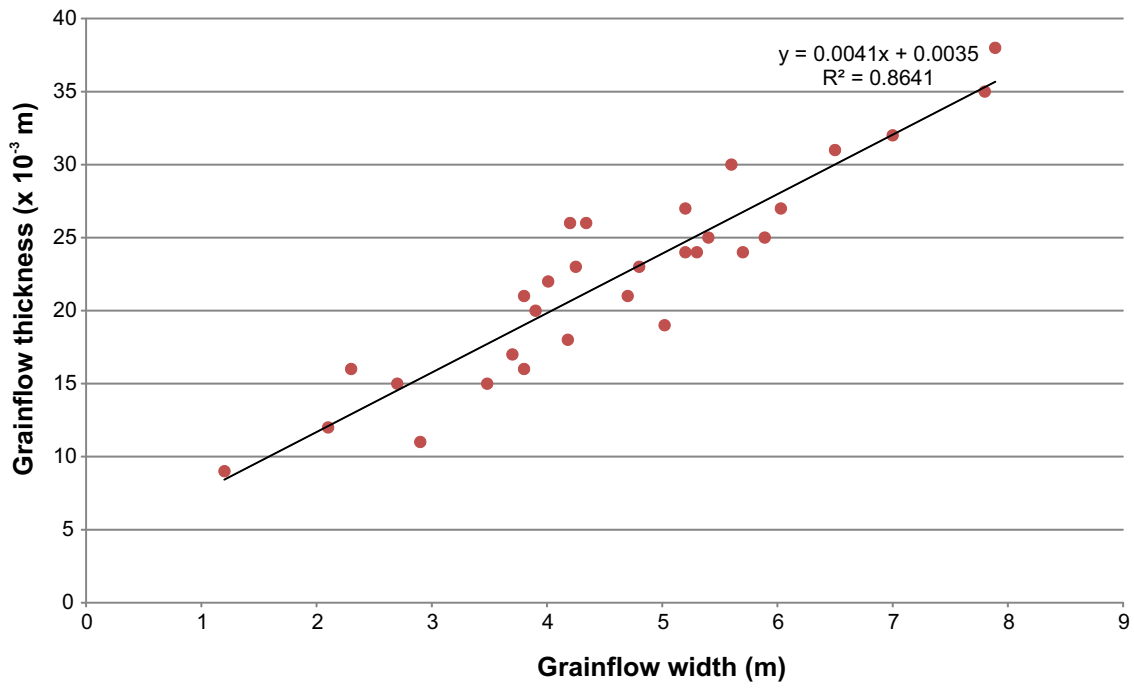
585 This research was funded by Areva, BHP Billiton, ConocoPhillips, Nexen, Saudi
586 Aramco, Shell and Woodside through their sponsorship of the Fluvial & Eolian
587 Research Group at the University of Leeds. Nathaniel Ball, Steven Banham and
588 John Wagner are thanked for their assistance with field data collection. We thank
589 Ryan Grimm, Lee Krystinik, and Colin North for their constructive and encouraging
590 reviews.

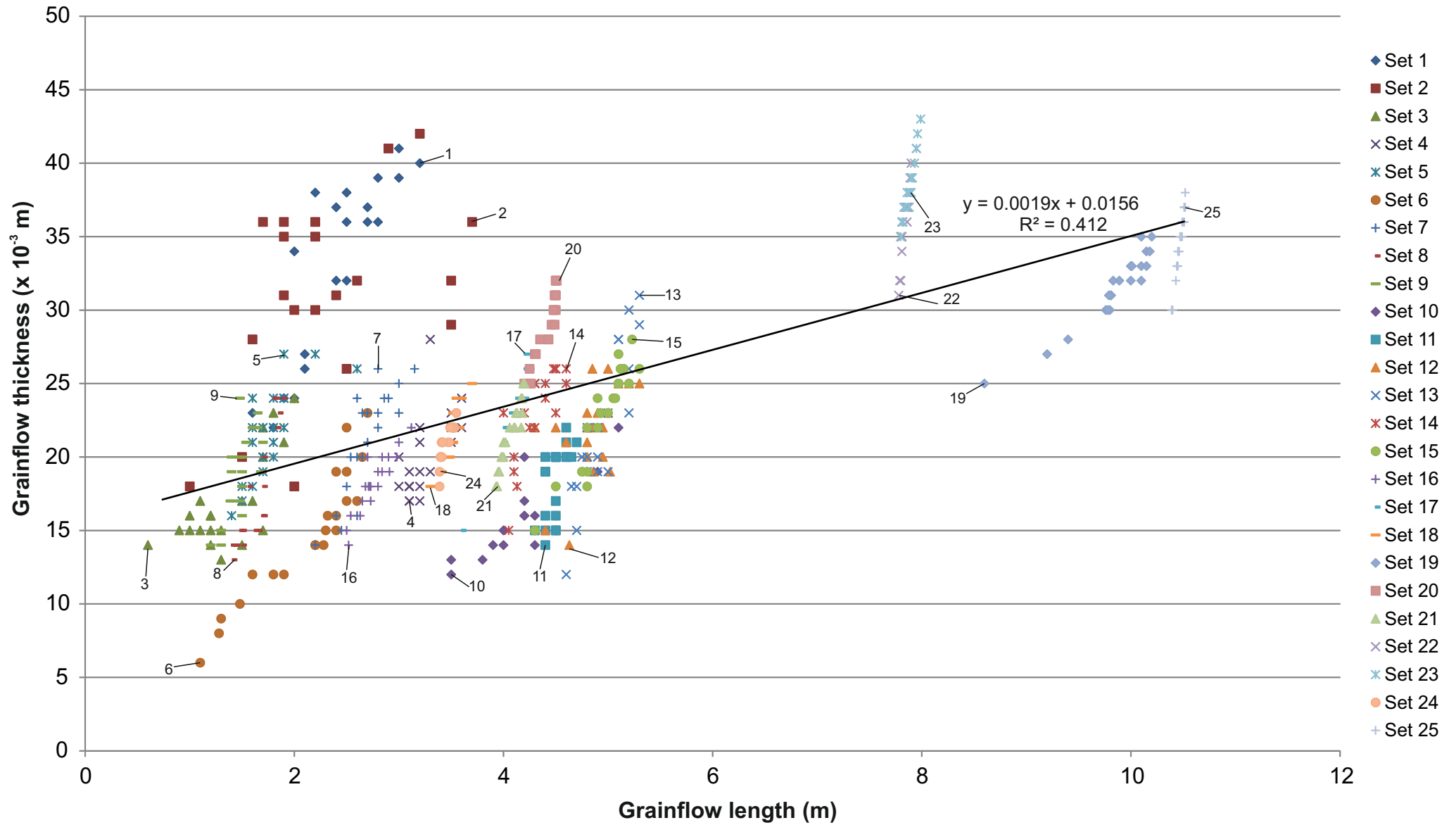


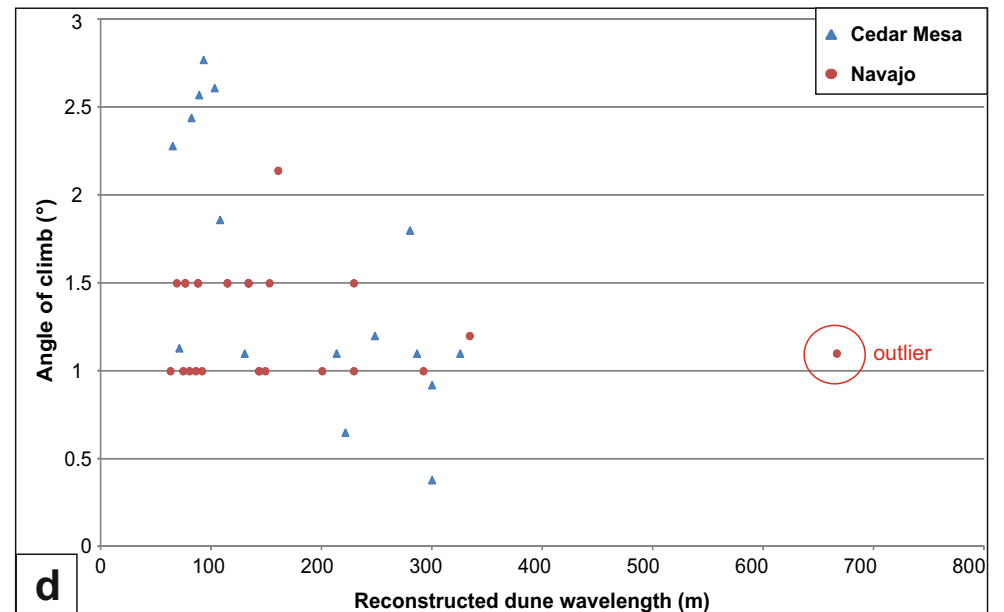
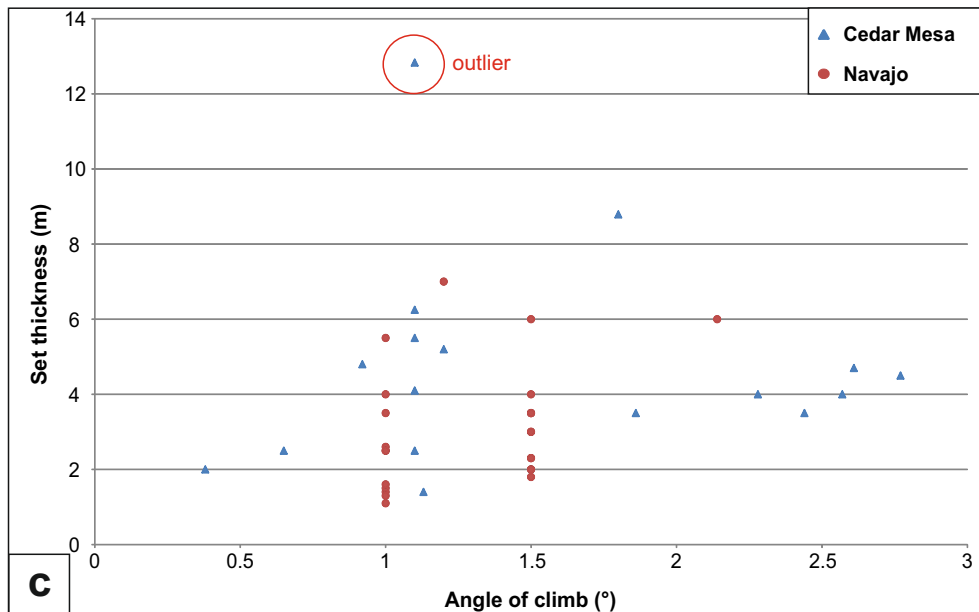
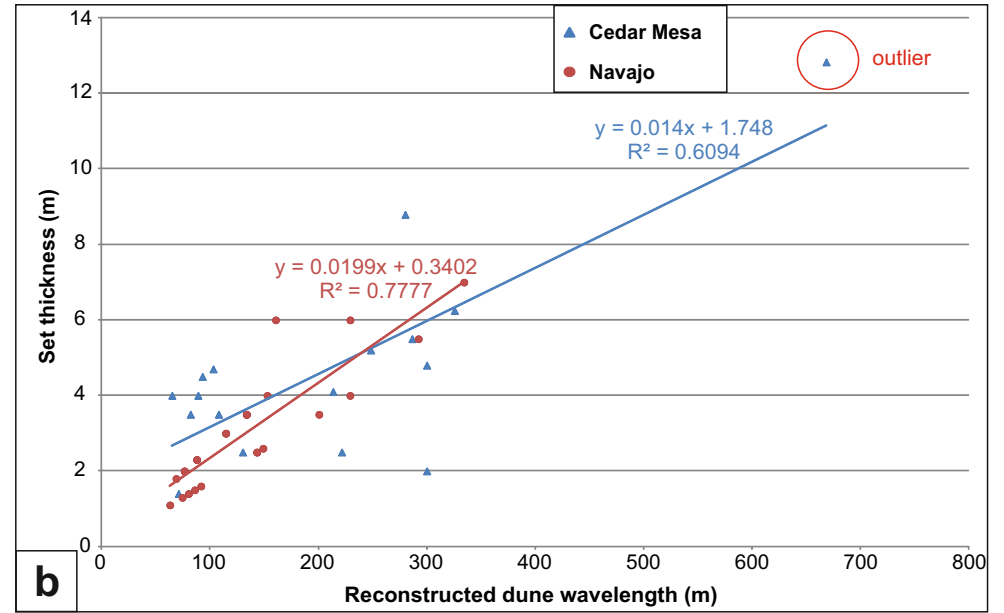
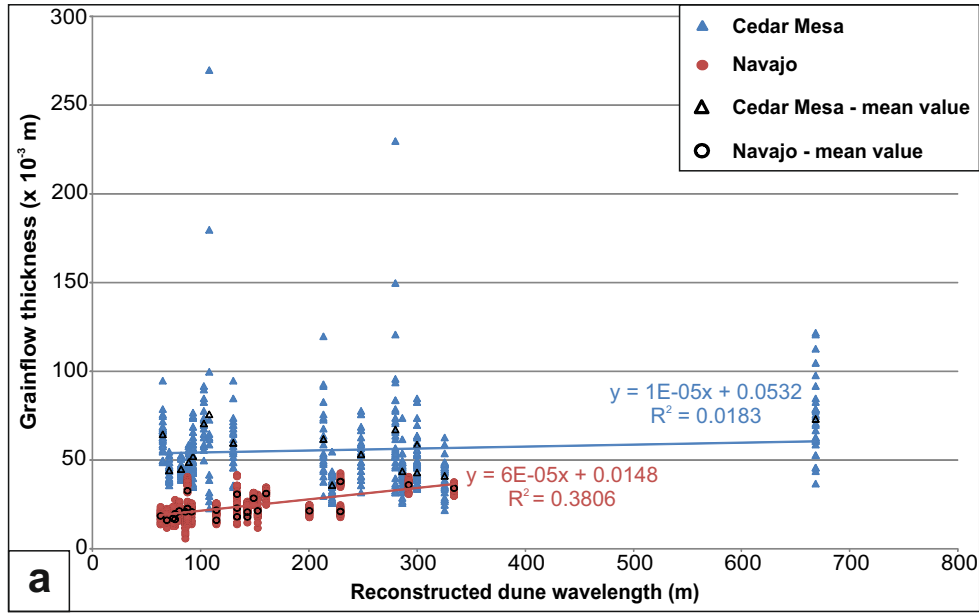


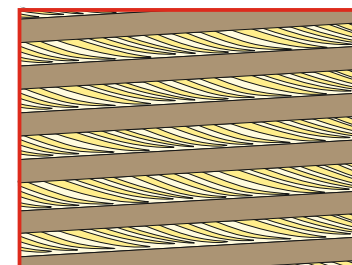
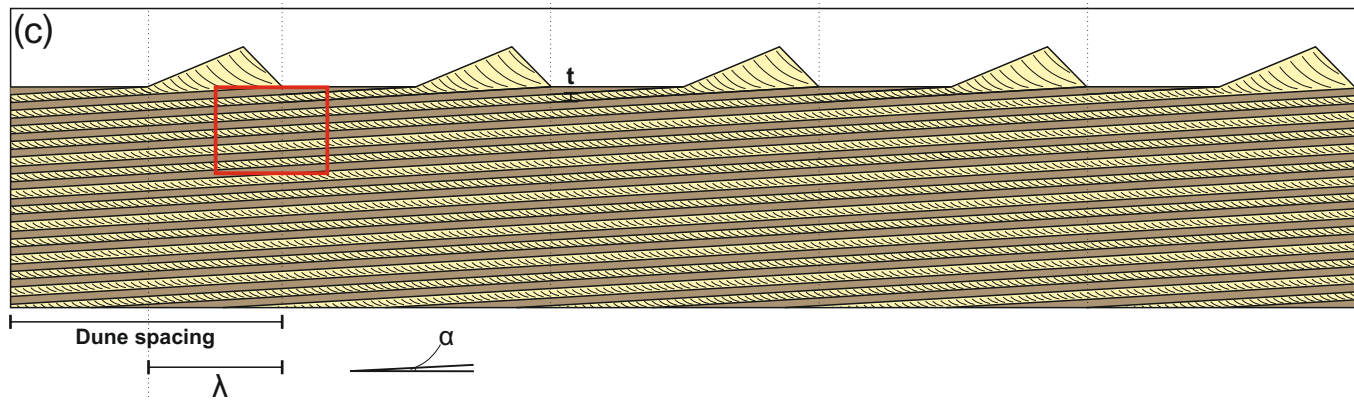
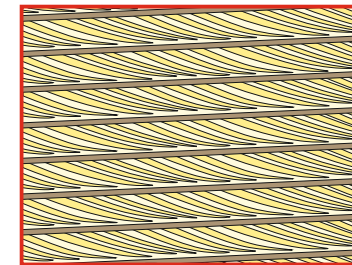
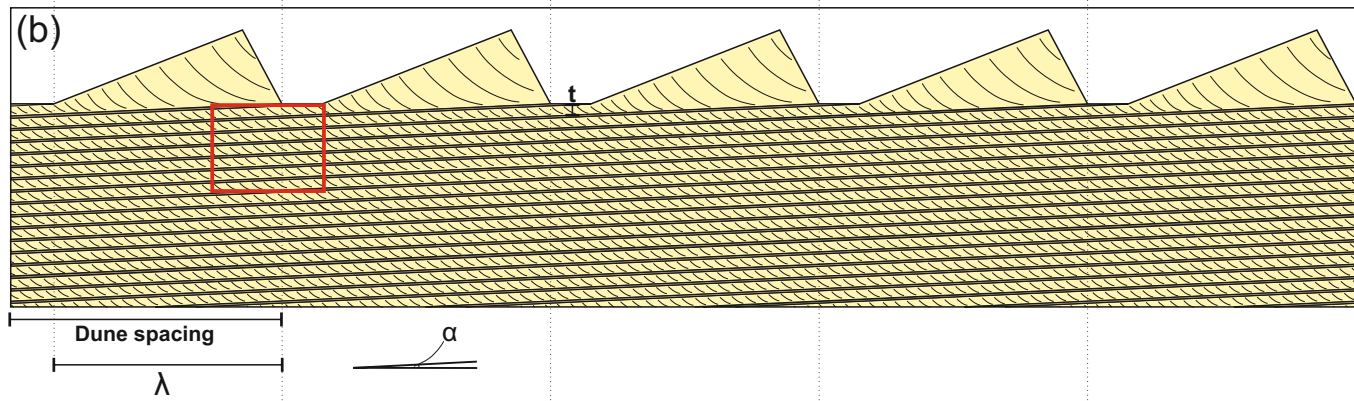
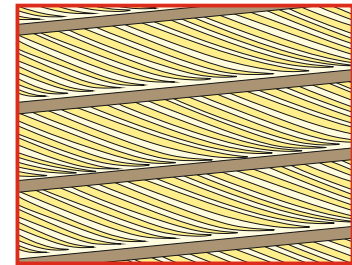
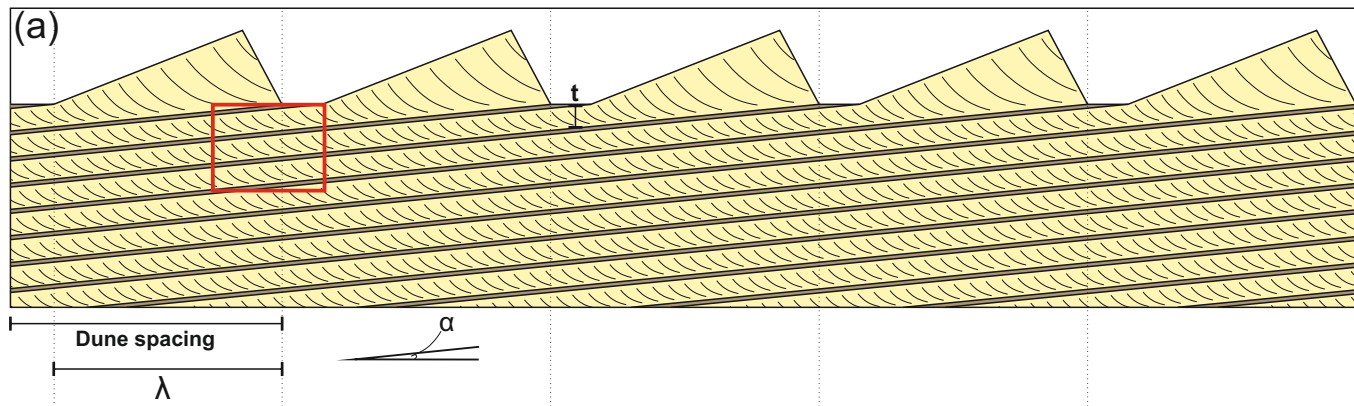


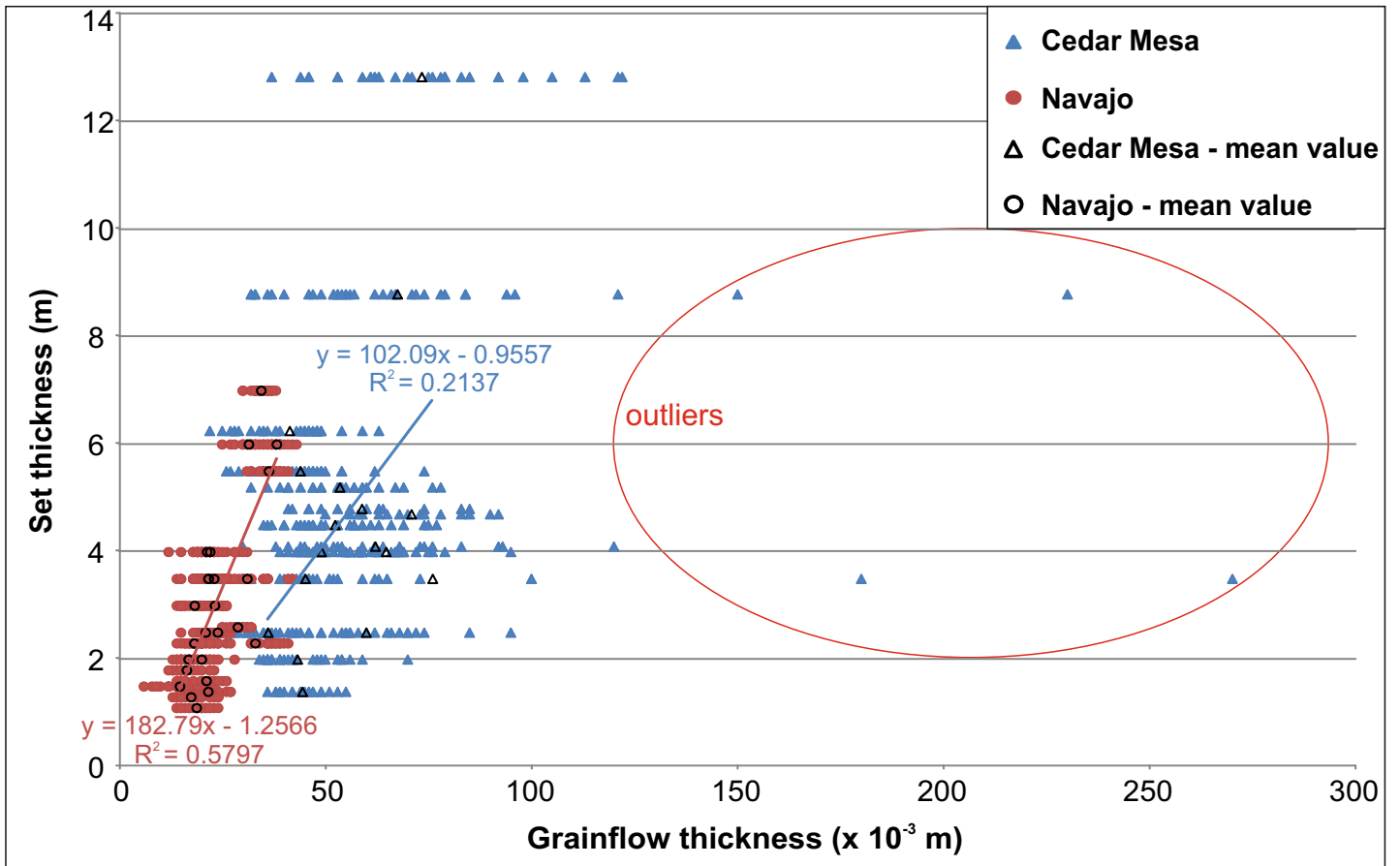




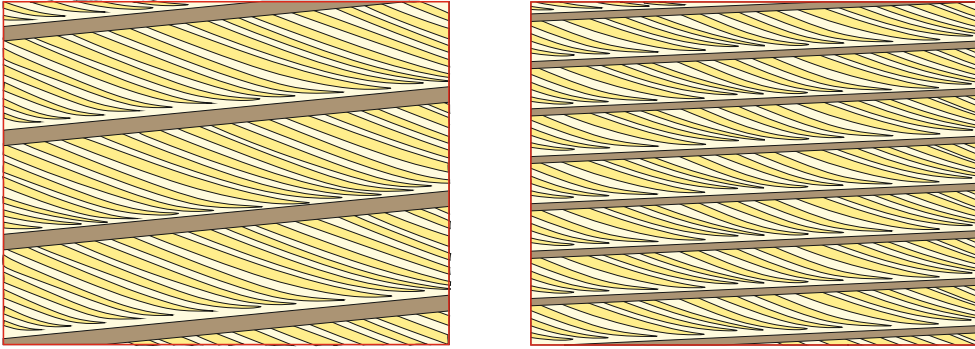




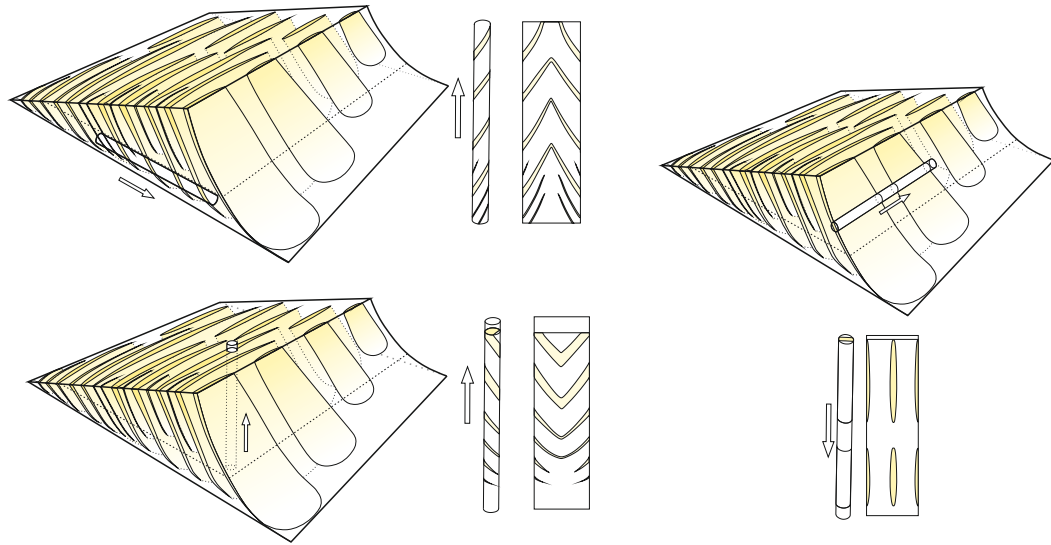




For a fixed dune wavelength, accumulation via migration at a steeper angle of climb (left) will generate and preserve thicker sets than for a less steep angle of climb (right)

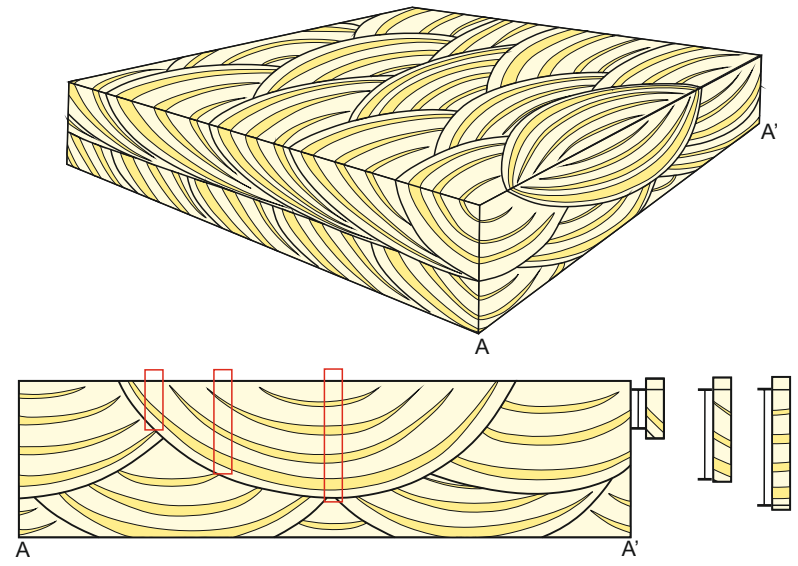


(a)

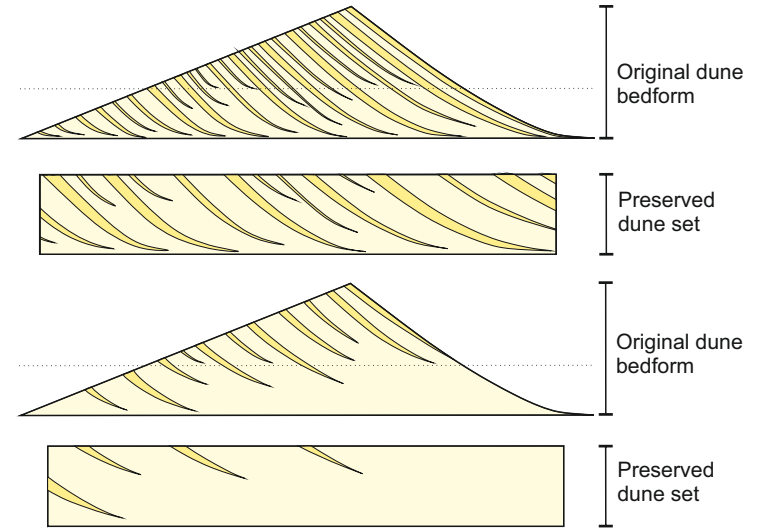


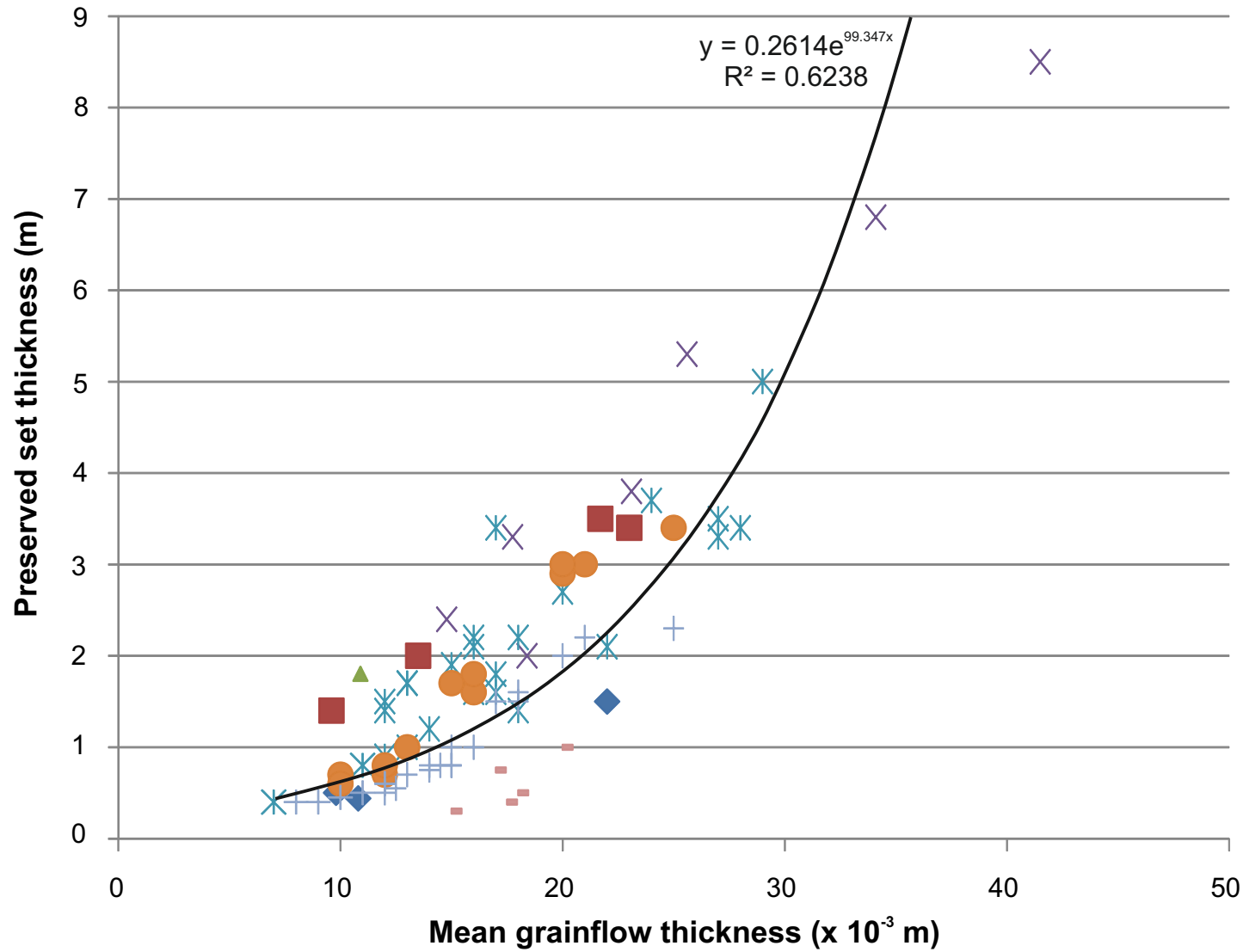
(c)

(b)



(d)





Eolian erg sequence

- ◆ White Canyon Seq B
- White Canyon Seq C
- ▲ White Canyon Seq E
- × White Canyon Seq G
- * Squaw Butte
- Salt Creek (U)
- + Salt Creek (L)
- Mosquito Butte

